JOURNAL OF PHYSICAL ORGANIC CHEMISTRY
J. Phys. Org. Chem. 2000; **13:** 719–728

Melting-points of the *meta*- and *para*-isomers of anisylpinacolone

Srinivasan S. Kuduva,[1] Jagarlapudi A. R. P. Sarma,[2] Amy K. Katz,[3] H. L. Carrell[3] and Gautam R. Desiraju[1]*

[1]School of Chemistry, University of Hyderabad, Hyderabad 500 046, India
[2]Molecular Modelling Group, Organic Division-I, Indian Institute of Chemical Technology, Hyderabad 500 007, India
[3]Fox Chase Cancer Center, 7701 Burholme Avenue, Philadelphia, Pennsylvania 19111, USA

Received 20 March 2000; revised 29 June 2000; accepted 3 July 2000

epoc ABSTRACT: The generally higher melting-point of a *para*-disubstituted benzene relative to the corresponding *meta*-isomer has been ascribed to the fact that, being more symmetrical, it can pack more tightly. Exceptionally, it was observed that whereas *m*-anisylpinacolone melts at 58.0 °C, the *para*-isomer melts lower at 39.5 °C. In this work we have attempted to understand this apparent anomaly. The crystal structures of both isomers were determined and the packing analysed. Energy calculations of the static structures and molecular dynamics (MD) simulations at temperatures just below the respective melting-points were performed. The structure analyses indicate that the intermolecular contacts are comparably weak in the two cases, and do not appear to be the direct cause of the melting-point difference. Thermal motion analysis, packing energies and MD simulations on minicrystals indicate the importance of both enthalpic and entropic factors in the melting behaviour of the two isomers. The higher melting point of the *meta*-isomer could originate from both a smaller ΔS_f and higher ΔH_f relative to the *para*-isomer. Copyright © 2000 John Wiley & Sons, Ltd.
Additional material for this paper is available from the epoc website at http://www.wiley.com/epoc

KEYWORDS: anisylpinacolone; melting-point; crystal structure; intermolecular interactions; packing energy; enthalpy; entropy; molecular dynamics

INTRODUCTION

Determination of melting-points is a simple experimental technique, used to establish compound purity, but the melting phenomenon itself has always been an enigma to structural chemists.[1–3] Can one correlate molecular structure with melting-point? If so, how? These questions have practical significance but are difficult to answer because the rationalization of a melting-point requires a thorough understanding not only of the strength and nature of the various intermolecular interactions in the crystal, but also of other factors such as the size, shape and symmetry of the molecule. However, some generalizations may be useful: (1) hydrogen bonding increases the melting-point; (2) the melting-point increases with increasing size of the molecule; (3) for disubstituted benzenes the *para*-isomer has a higher melting-point than the *meta*-isomer. The hydrogen bond is a strong intermolecular interaction and is highly electrostatic, even with some covalent character. Therefore, it is associated with an increase in melting-point. An increase in molecular size will lead to an increase in the van der Waals interactions and this results in a higher melting-point. Finally, the relatively more symmetrical *para*-isomer of a disubstituted benzene supposedly packs more

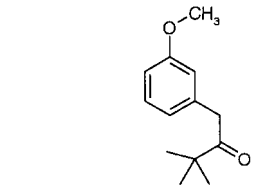

1

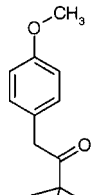

2

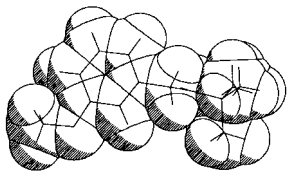

1

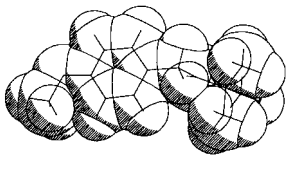

2

**Correspondence to:* G. R. Desiraju, School of Chemistry, University of Hyderabad, Hyderabad 500 046, India.
E-mail: desiraju@uohyd.ernet.in
Contract/grant sponsor: NIH; *Contract/grant number:* CA10925.

Table 1. Some crystallographic details for the isomers of anisylpinacolone

Parameter	**1** (*meta*)	**2** (*para*)
Empirical formula	$C_{13}H_{18}O_2$	$C_{13}H_{18}O_2$
Formula weight	206.27	206.27
Crystal system	Orthorhombic	Monoclinic
$F(000)$	448	224
a (Å)	5.980(4)	9.4670(19)
b (Å)	13.766(3)	6.2700(13)
c (Å)	14.103(2)	9.905(2)
β(°)	90	91.92(3)
V (Å)	1161.0(8)	587.6(2)
Z	4	2
Space group	$P2_12_12_1$	Pc
D_c (g cm^{-3})	1.180	1.166
Temperature (K)	120(2)	120(2)
Radiation	Mo Kα (0.71073 Å)	Mo Kα(0.71073 Å)
Reflections measured	5184	4505
Range of θ (°)	3.0 –27.5	3.0 –27.5
Range of h; k; l	−7 to 7; −17 to 17; −18 to 18	−12 to 12; −8 to 8; −13 to 10
Unique data	1532	1326
Observed data	1109	1051
No. of refined parameters	136	136
R(int)	0.00	0.00
Goodness of fit	1.063	1.024
$R1$	0.0517; 0.0776	0.0449; 0.0562
R_w	0.1090; 0.1336	0.0940; 0.0977
Percentage of filled space	69.6	67.9

tightly than the corresponding *meta*-isomer and, as a result, the melting-point of the *para*-isomer is generally higher.[2]

As an exception to the last 'rule,' it was noted that for anisylpinacolone, the *meta*-isomer, **1**, has a higher melting-point (58.0 °C) than the *para*-isomer, **2** (39.5 °C). This study is an attempt to correlate these 'anomalous' melting points.[4] Some possible questions that could be posed are the following: (1) is it the lower melting-point of the *para*-isomer or the higher melting-point of the *meta*-isomer that is unusual?; (2) are these melting-points really anomalous or is the usual *meta–para* rule for melting-points inappropriate for these compounds? To investigate these matters further, the crystal structures of the two isomers were determined.

The melting phenomenon is associated with both enthalpic (ΔH_f) and entropic (ΔS_f) changes. At the fusion temperature, $\Delta H_f = T_f \Delta S_f$. Information about crystal enthalpy is derived in a straightforward way from the x-ray positional parameters in the absence of any disorder. Despite the fact that this 'static' structure is actually a time- and space-averaged structure, these averaged positional parameters may be used to evaluate crystal enthalpies directly. Entropic factors arise necessarily out of disorder or implicitly through differences, mainly in the premelting stage, that arise from: (1) molecular rotational and translational motions and (2) multiple preferred orientations. Information about crystal entropy may be obtained indirectly by examining trajectories in molecular dynamics (MD) simulations.

For flexible molecules, the process of randomization of molecular conformations in melting constitutes a mode of disordering distinct from and additional to positional and orientational disorder and is expressed by

$$\Delta S_f = \Delta S_{pos} + \Delta S_{or} + \Delta S_{confor} + \ldots \quad (1)$$

The heat of fusion, ΔH_f, and entropy of fusion, ΔS_f, are related to the fusion temperature by

$$T_f = \Delta H_f / \Delta S_f = \Delta H_f / (\Delta S_{pos} + \Delta S_{or} + \Delta S_{confor} + \ldots) \quad (2)$$

When two molecules of similar shape and size have comparable crystal packing arrangements, differences in the positional and orientational contributions to ΔS_f are small and conformational contributions to the entropy could result in melting-point variations.

Packing energy calculations, thermal motion analysis and molecular dynamics studies were undertaken for **1** and **2** and, based on the above equations, the enthalpic and entropic factors were evaluated.

EXPERIMENTAL

Both **1** and **2** were synthesized according to literature methods.[4] **1**: ^{1}H NMR (200 MHz, $CDCl_3$), δ 1.18 (s, 9H), 3.78 (s, 2H), 3.80 (s, 3H), 6.68–7.27 (m, 4H); IR (cm^{-1})

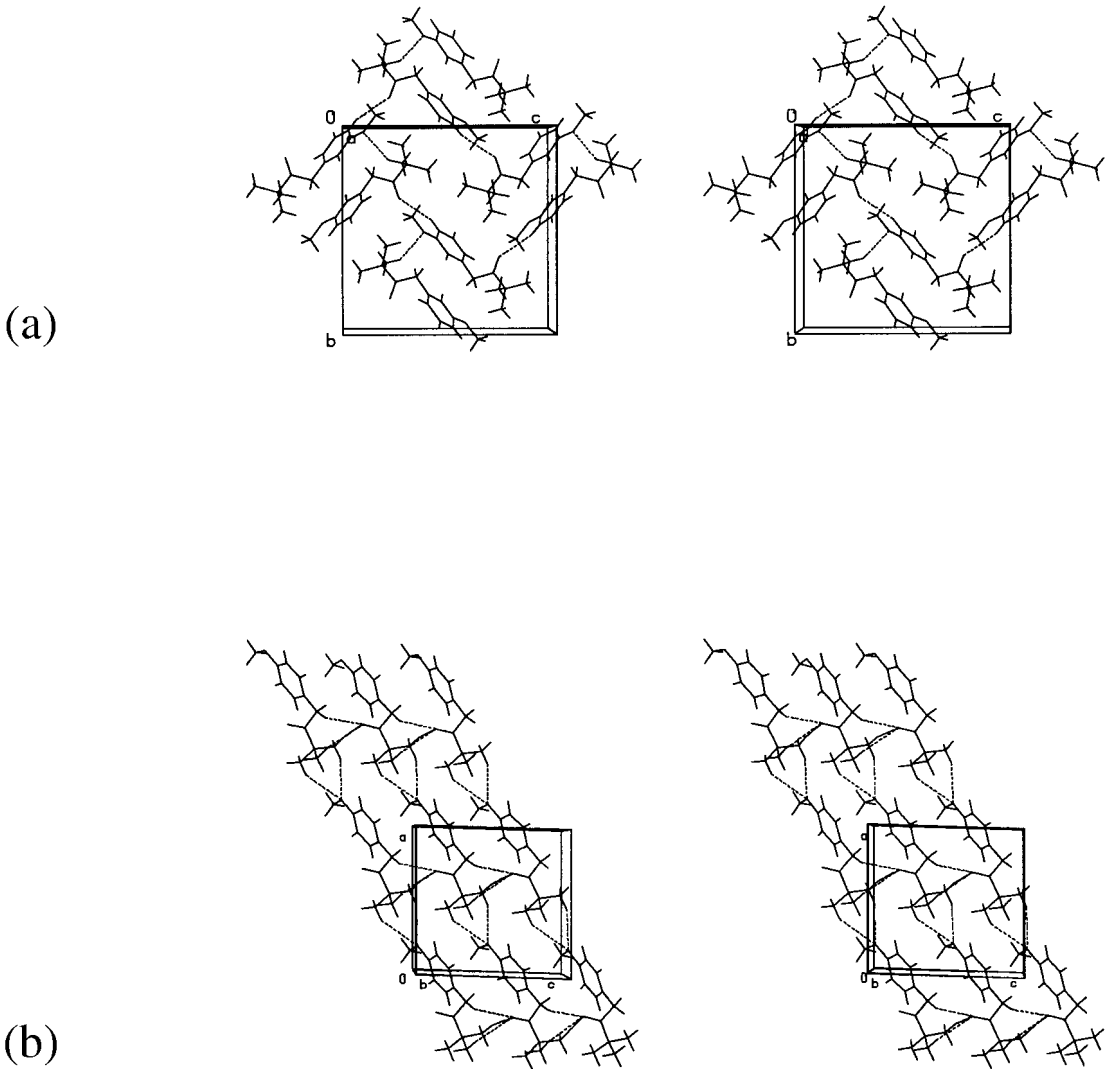

Figure 1. (a) Stereoview of the crystal packing of **1** down [100] with intermolecular contacts in dotted lines. (b) Similar stereoview of the crystal packing of **2** down [010]

2996, 1709, 1466, 1265, 1153, 1053, 767. **2**: ^{1}H NMR (200 MHz, $CDCl_3$), δ 1.2 (s, 9H), 3.78 (s, 2H), 3.80 (s, 3H), 6.8–6.9 (d, 2H), 7.1–7.2 (d, 2H); IR (cm^{-1}), 2966, 1709, 1512, 1487, 1248, 1179, 1034, 820. Single crystals of **1** were obtained easily from *n*-hexane at $-20\,°C$. However, a pure sample of **2** did not yield good single crystals from any of the common solvents or solvent mixtures. Finally, single crystals were obtained by slowly cooling the crude material (as obtained in the reaction) from 40 to 0 °C. X-ray single-crystal diffraction data for **1** and **2** were collected at 120 K with an Enraf Nonius FAST area detector.

The structures were determined by direct methods and refined by full-matrix least-squares on F^2 using SHELX97.[5] All the non-hydrogen atoms were refined anisotropically and the hydrogen atoms which were initially selected from the Fourier map were fixed with the AFIX routine in the later stages of the refinement. For the calculations of intermolecular contacts and energies, the hydrogen atom positions were normalized at a C—H distance of 1.083 Å. The crystal structures were analyzed with PLATON.[6] Other salient features of the crystal structure determinations are given in Table 1 and Fig. 1. Some of the intermolecular contacts are given in Table 2. Rigid body thermal motion analysis was carried out with the program THMA11.[7]

Computational methodology

Molecular parameters (dimensions, area, volume) and crystal parameters (packing coefficients, packing potential energies) for both isomers were calculated. In these calculations, the x-ray structures were used as the starting point. Partial charges were obtained from charge equilibrium methods and packing energies were

Table 2. Intermolecular interactions[a]

Isomer	Interaction	H···A (Å)d	D···A (Å)D	D—H···A (°)θ
1 (*meta*)	C—H···O	2.67	3.70	160
	C—H···O	2.74	3.43	121
	C—H···O	2.59	3.58	150
	C—H···O	2.95	3.57	117
	C—H···O	2.61	3.52	141
	C—H···O	2.84	3.72	139
	C—H···O	2.53	3.26	124
	C—H···π	2.87	3.93	164
	C—H···π	2.98	4.05	170
2 (*para*)	C—H···O	2.52	3.46	144
	C—H···O	2.62	3.63	155
	C—H···O	2.84	3.84	153
	C—H···O	2.85	3.85	153
	C—H···O	2.80	3.76	148
	C—H···π	2.63	3.41	129
	C—H···π	2.94	3.88	145

[a] For C—H…O interactions, the accepted ranges are d, 2.00–3.00Å, D, 3.00–4.00Å, θ, 110–180°, with both distance and angle attributes assessed concurrently (see ref. 9, pages 44–66).

calculated using the Burchart–Dreiding force field[8] with explicit inclusion of all types of hydrogen bonds defined by 2.9 Å distance and 130° angle criteria.[9] Further, the experimental bond lengths and angles were optimized with MOPAC employing AM1 methods.[10] Torsion angles were not varied and the experimental conformation thus retained in the optimized geometry. Partial charges obtained from these calculations were

Table 3. Details of molecular and crystal parameters, packing energies and molecular dynamics simulation results in the premelt stage for **1** and **2** (all energies in Kcal mol^{-1})

Parameter	**1**			**2**		
Molecular parameters						
Molecular dimensions (Å)	13.099, 7.781, 6.634			13.757, 7.277, 6.304		
Molecular volume (Å)^3	218.0			217.4		
Surface area (Å)^2	261.4			260.5		
Heat of formation	−69.88			−69.80		
Dipole moment (D)	2.103			3.116		
Crystal parameters						
Melting point (K)	331			312.5		
Density (g cm^{-3})	1.18			1.166		
Libration (inertial) (°)^2	13.16, 1.76, 0.35			13.11, 1.56, −0.86		
Translation (inertial) (Å)^2	0.1517, 0.1363, 0.1181			0.1757, 0.1537, 0.1319		
Packing coefficient	0.784			0.772		
Packing energy	−38.33[a]	−28.45[b]	−28.59[c]	−37.22[a]	−26.69[b]	−27.36[c]
VdW	−23.86	−22.34	−22.42	−23.96	−20.96	−21.52
Columbic	−13.00	−4.99	−4.96	−12.16	−4.56	−4.49
H-bond	−1.47	−1.12	−1.21	−1.10	−1.17	−1.35
Molecular dynamics[d]						
Temperature (K)	323.4	332.8	327.0	294.6	312.3	307.8
Pressure	1.674	1.709	1.693	1.845	1.871	1.858
Stress	−0.013	0.013	0.000	−0.016	0.006	−0.004
Total energy	73.87	73.91	73.90	70.73	70.78	70.74
Kinetic	31.81	32.73	32.16	28.98	30.72	30.28
Potential	41.14	42.09	41.74	40.01	41.80	40.47
Valence	36.21	37.27	36.72	34.14	35.86	34.75
Non-bonded	4.636	5.289	5.020	5.436	6.016	5.717
VdW	13.76	14.40	14.14	14.80	15.40	15.08
Coulombic	−9.172	−9.084	−9.124	−9.399	−9.323	−9.361

[a] Packing potential energy and its contributors with x-ray observed geometry along with partial charges derived from the charge equilibrium methods.
[b] Packing potential energy and its contributors as obtained when the x-ray observed bond lengths and angles were optimized with AM1 methods and using derived partial charges. Molecules were held at the same positions as observed in the crystal.
[c] Packing potential energy with geometry and charges as in footnote b. However, the molecules were considered as rigid bodies and were optimized with respect to rotational and translational motion in the cell with constant volume.
[d] The three columns for each structure refer to the minimum, maximum and average values, respectively, in the MD run.

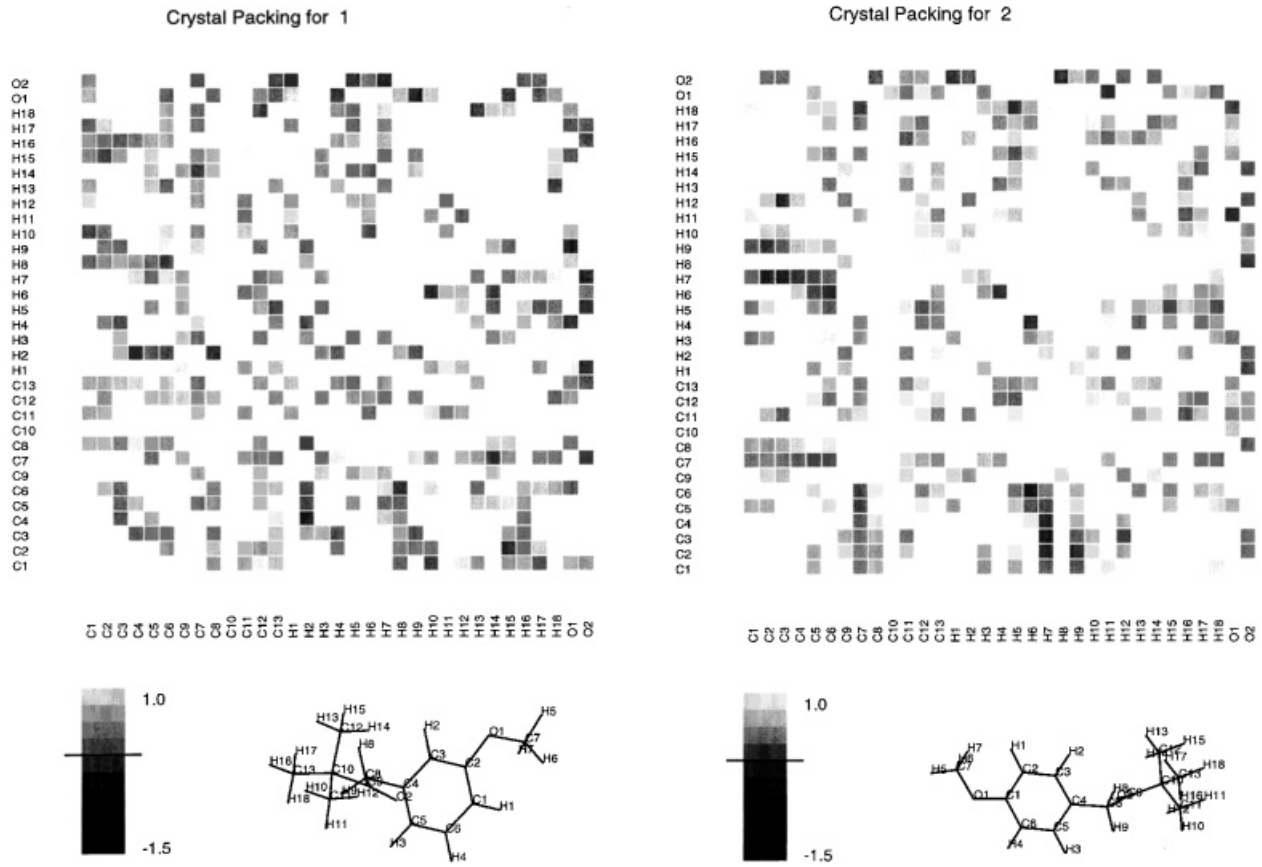

Figure 2. NIPMAT representation of intermolecular contacts in **1** (left) and **2** (right) The grey intensity indicates the strength of the intermolecular contact with respect to the distance. The similarity in the grey scale and density of squares in the two plots shows that the two crystal packings are comparable

also used to calculate the electrostatic contribution to the packing energies with the explicit inclusion of hydrogen bonds. The molecules were considered as rigid bodies and varied with respect to the translations and rotations along the Eulerian axes in the fixed cell during the energy minimization. The experimental crystal symmetry was always retained. Various energies along with the molecular and crystal parameters are given in Table 3.

For the MD study involving minicrystals, the structural information for both isomers was read into the Cerius[2] molecular modelling software (Molecular Simulation, San Diego, CA, USA). Minicrystals (supercell) comprising $6 \times 3 \times 3$ unit cells (216 molecules) and $4 \times 8 \times 4$ unit cells (256 molecules) of **1** and **2** respectively were considered in the space group $P1$.[11] These minicrystals were considered as periodic systems in all the MD simulations. The Burchart–Dreiding force field was employed. Partial atomic charges for all the atoms in the minicrystals were assigned by the Gasteiger method. Electrostatic interactions were treated by the Ewald summation method as this is a better way of estimating the long-range interactions. Initially, the individual molecules in the supercell were considered as rigid bodies and the minicrystal was minimized without varying the cell parameters. This was done until the gradient or the energy between two successive cycles was less than the default threshold limit. A full minimization of all atoms at constant volume then followed. This reminimization is necessary to normalize the bond parameters to those corresponding to the force fields. Such an exercise is necessary before the start of an MD study. However, and satisfactorily, the minimization did not produce any significant conformational or packing changes.

MD analysis at constant volume and energy used the Verlet leapfrog integrator with a 1 fs time step.[11,12] The initial atomic velocities were assigned based on a Boltzmann distribution at a temperature 5 °C below the respective melting-points. The trajectory data including atomic velocities and coordinates were saved at a frequency of 0.5 ps. The MD simulations for both isomers were performed for a duration of 10 ps after an equilibration run of 1 ps in each case. In an Octane SGI workstation with an R10000 processor, each simulation lasted around 5 days. Three different MD runs, at 308 K for **1** and **2** and at 326 K for **1**, were carried out. For reference, the melting-points of **1** and **2** are 331 and 312.5 K, respectively.

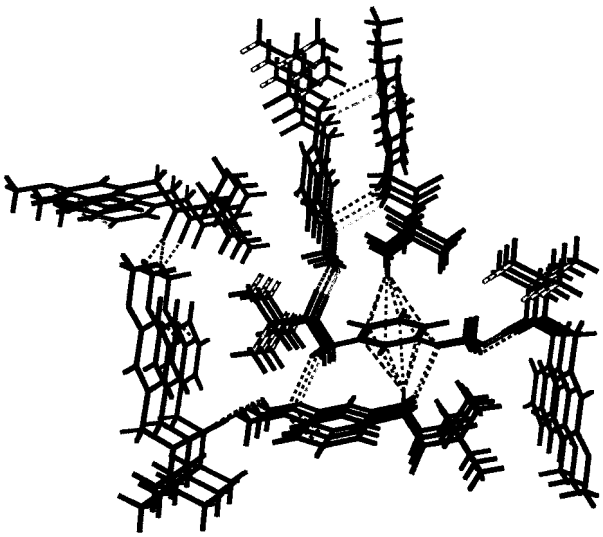

Figure 3. A molecule of **1** (centre) and its neighbours showing C—H···O and C—H···π contacts. The carbonyl O-atom forms C—H···O contacts with two different methoxy H-atoms and the methoxy O-atom interacts with one of the methylene and aromatic H-atoms. The other methylene H-atom and the one of the H-atoms of the *tert*-butyl group are involved in C—H···π contacts on either side of the phenyl ring and occupy two vertices of two symmetrical cones

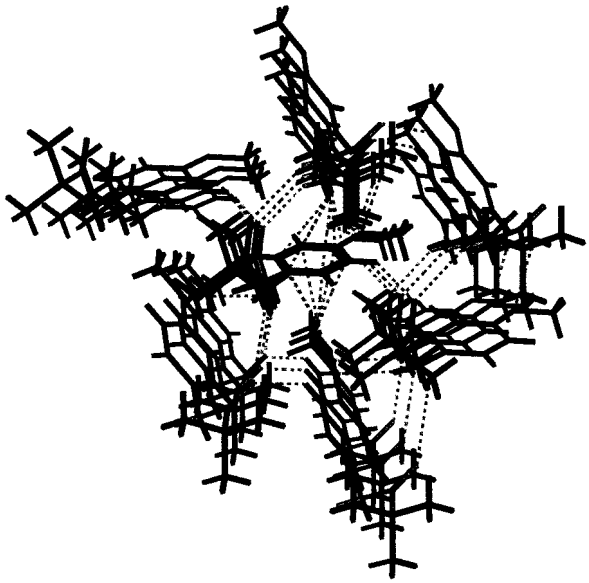

Figure 4. A molecule of **2** (centre) and its neighbours showing C—H···O and C—H···π contacts. Compare this with Fig. 3. Different modes of intermolecular contacts and symmetrical and unsymmetrical C—H···π interaction cones are clearly observed. For instance, the carbonyl O-atom interacts with an aromatic and one of the methylene H-atoms and the methoxy O-atom interacts with the two tert-butyl H-atoms. Note also that the methoxy and one of the methylene H-atoms which form C—H···π contacts are unsymmetrically positioned at the vertices

RESULTS AND DISCUSSION

Crystal packing

The melting-points of **1** and **2** were confirmed with differential scanning calorimetry (DSC) (0–100 °C). The DSC traces did not indicate the existence of any other crystalline phase or possible phase transitions before melting. The difference in melting-points is around 6% of the mean melting temperature. This is significantly higher than that observed for simple *meta–para* pairs of non-polar substituted benzenes, wherein the *para*-isomer is almost always the higher melting (one of the exceptions being isophthalic acid, m.p. 342 °C, and terephthalic acid, m.p. 301 °C).[2]

Both title isomers of anisylpinacolone adopt non-centrosymmetric space groups and crystallize with one molecule in the asymmetric unit. The crystal structures are shown in Fig. 1. Both structures contain weak C—H···O and C—H···π hydrogen bonds.[9,13,14] These interactions are formed between glide-and translation-related molecules in **2** and between 2_1-related molecules in **1**. Pertinent interatomic distances are given in Table 2. Both crystal structures were further analyzed with the use of an interactive display program, NIPMAT.[14] The 2-D NIPMAT pictorial representations of the structures are shown in Fig. 2. These plots show that the overall packing is very similar in the two structures.

Both ketones **1** and **2** contain similar C—H hydrogen bond donors (aromatic, methylene, methoxy, methyl) and acceptors (carbonyl, methoxy, aromatic ring), but the intermolecular contacts are slightly different. These minor differences could be attributed to the difference in the dipole moment (Figs 3 and 4). Although these interactions have some directional preference, they are rather long and could be considered to be very weak. In general, the crystal packing in both isomers is very similar. Hence it is difficult to correlate the melting-point difference of ~20 °C in the two isomers with their crystal structures. In order to quantify the enthalpic contributions in the structures, the packing potential energies comprising van der Waals, Coulombic and hydrogen bonding energies were next computed.

Packing potential energies

Packing coefficients and potential energies of the two isomers are given in Table 3. The *meta*-isomer has a slightly higher packing coefficient and experimental density. For the energy calculations, different molecular geometries (x-ray, MOPAC-optimized) were used. Although the different methods that were used to calculate partial charges result in some variation in the Coulombic contributions, the energies of the *meta*- and *para*-isomers (and therefore the differences in these energies) are virtually the same for any given method. Even the component terms to the overall energy (van der Waals, Coulombic and hydrogen bond) are comparable.

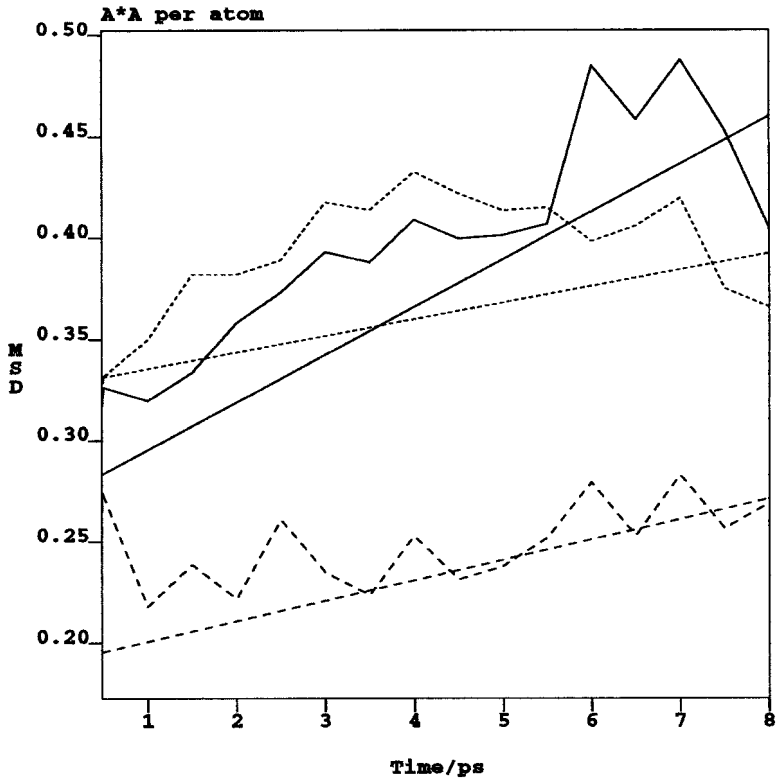

Figure 5. Variations of the mean square displacements (MSD) with time for a cluster of four molecules in the centre of the minicrystals. Dashed lines and dotted lines indicate the MD simulations at 308 K for **1** and **2**, respectively, and solid lines represent the simulation at 326 K for **1**. The polygons indicate the actual variations and the straight lines are the corresponding least-squares fits. For **1**, the MSD are comparatively low at 308 K. The increase in the slope of the least-squares fit line at 326 K is clearly seen for **1**

This is so not only because the same force field (Burchart–Dreiding) is being used everywhere, but also because the intermolecular interactions in the two structures are nearly the same. Consistently, however, the *meta*-isomer, **1**, has a slightly lower potential packing energy than the *para*-isomer, **2** (-1.2 kcal mol^{-1}). Since this result corroborates its slightly higher packing coefficient and density, it was concluded that this small enthalpic difference could contribute in part to the difference in the melting-points of the two isomers.

Molecular dynamics

To the extent that entropy connected inferences may be drawn from a visual examination of MD trajectories, MD studies were carried out on minicrystals so as to assess the entropic influence on the difference in the melting-points. These studies were carried out on minicrystals, and have been used previously to study cooperative effects.[11] In the absence of any direct evidence for disorder in the native structures, they can provide some quantification for crystal entropy effects.[2] These MD calculations are very time consuming because a large number of atoms in a periodic system have to be considered. However, a 10 ps dynamics run gave satisfactory results in that the equilibrium with respect to the total energy was reached within an initial run of 0.5 ps. Based on our experience with other similar studies involving minicrystals,[11] we realized that longer simulations do not necessarily produce different results *if the relative molecular motion is the only item of interest*. Various minimum, maximum and average energies, and the temperature, during the MD runs are given in Table 3. The total energy is the sum of kinetic and potential energies. The latter, in turn, has contributions from valence bond and non-bonded terms. The non-bonded energy has van der Waals and Coulombic contributions and follows a similar trend as seen in the crystal packing energy calculations; in other words, it is slightly lower for **1**. The important distinction between crystal packing potential energy and the potential energy in an MD run is that while the former consists of only intermolecular energies, the latter contains all types of interatomic energies. The variations with time of the mean square displacements (MSD) for a molecule in the middle of the minicrystal are plotted for the three different MD runs in Fig. 5. At 308 K, the molecular motion in **1** is clearly less than that in **2**. In the premelting stage, the molecular motions of **1** and **2** with time are nearly comparable with a moderately enhanced motion for **1**. However, the MSD motion is the result of combined rotational and translational motions. Since the

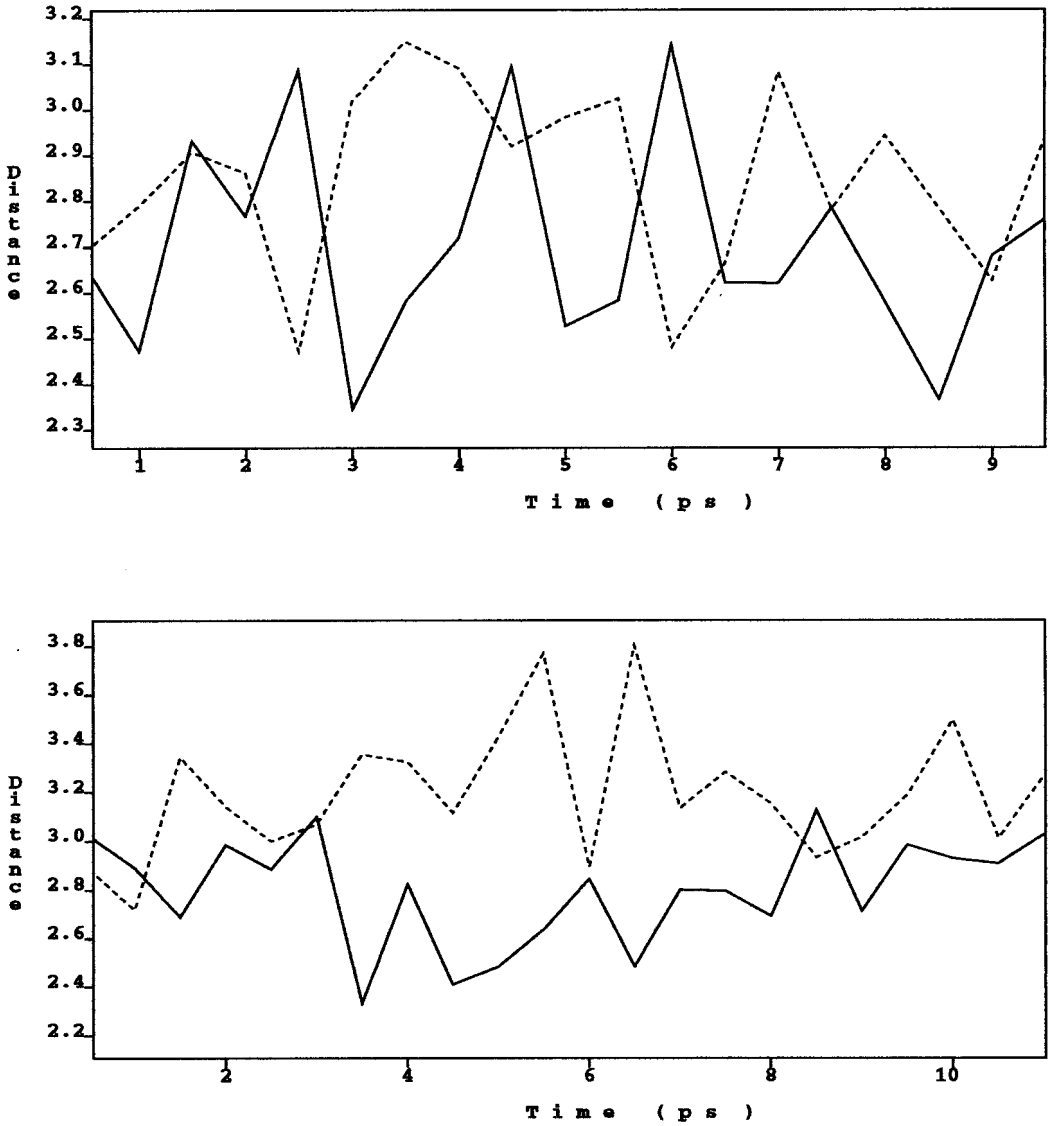

Figure 6. Variations in the two different C—H···O interactions (solid and dotted lines) of the carbonyl group in the premelting stage. MD simulations are shown for **1** (top) and **2** (bottom)

x-ray data were collected at 120 K and the refinements of positional parameters and ADPs were highly satisfactory, a rigid body thermal motion analysis was carried out (Table 3). This analysis indicates a definitely higher translation motion for **2** with a slightly enhanced librational motion for **1** even at 120 K. Such motions could be further amplified at higher temperatures, especially near the melting-point. Fig. 5 shows that these motions are clearly observed at 308 K, when the motion in **1** is less than that in **2**. In short, the thermal motion analysis is in agreement with the MD runs.

The variations in the C—H···O interactions[9,14] in the premelting stage are also of interest (Fig. 6). Interactions between the carbonyl O-atom and two different H-atoms in **1** [Fig. 6(a)] and **2** [Fig. 6(b)] are plotted. All these C—H···O interactions are weak. However, Fig. 6(a) shows that at any instant there is a preference for one of these C—H···O interactions (either dotted or solid line at any given instant) to be shorter than the other. This could result from a carbonyl group motion in which two very closely separated, yet individually preferred, orientations are generated. However, in **2** [Fig. 6(b)] such a switching between two preferred positions is not observed during the MD run—the carbonyl group prefers to remain close to only one of the H-atoms. Similar results were obtained when the C—H···O interactions involving the methoxy O-atoms were analysed.

The motions of atoms/molecules along with their internal rotations, vibrations and molecular librations and translations in the crystal were obtained by superposition of a molecule at regular time intervals during the run. In Figs 7 and 8, these motions between three selected molecules in the premelting stage are shown for **1** and **2**, respectively. The three molecules were chosen such that

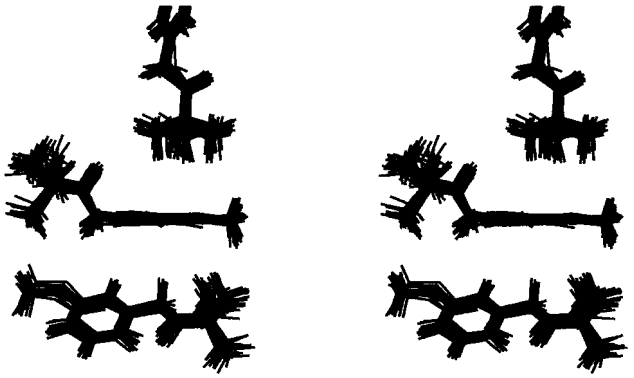

Figure 7. Motion of the three molecules of **1** optimizing C—H···π interactions (MD results). Note the relatively smaller translational motion for the molecules in the middle

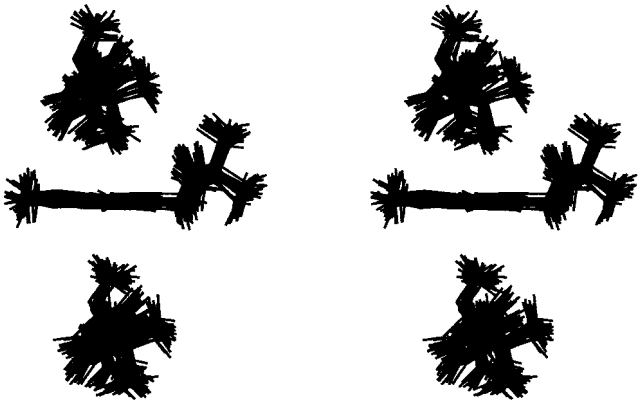

Figure 8. Motion of the three molecules of **2** optimizing C—H…π interactions. Note the slightly enhanced translational motion and the near random orientation of the methoxy groups with the concomitant loss of C—H…π interactions

C—H···π contacts may be visualized in both cases. In the static crystal structures these contacts are well oriented in **1** and to a lesser extent in **2** (Figs 3 and 4). During the MD run for **1**, the methylene and methyl H-atoms (Fig. 7) that contribute to the C—H···π contacts do not move significantly whereas in **2** (Fig. 8), the methoxy group which is involved in such contacts is randomly oriented, losing the interaction and/or its specificity almost completely. The slightly enhanced MSD values observed for **1** (Fig. 5) could arise from the higher librational motion of a molecule (or a part of it) so that some specific intermolecular contact is optimized. In summary, the alternation in C—H···O geometries between two comparable situations in **1** could well increase the entropy, thereby lowering ΔS_f and increasing the melting-point. In **2**, such a possibility is absent and the melting-point is lower. If the calculated packing potential energy difference between **1** and **2** (1.23 kcal mol^{-1}) in the minimized structures is taken as being equal to $\Delta(\Delta H_f)$, the entropy of fusion, $\Delta(\Delta S_f)$, will be approximately 1.22 cal K^{-1} mol^{-1}, reflecting the differences in molecular motion in these two systems.

CONCLUSIONS

The difference in the melting-points of the *meta*- and *para*-isomers of anisylpinacolone may be rationalized in terms of enthalpic and entropic contributions to the melting-event. Single-crystal x-ray structural analysis and packing potential energy calculations reveal that the *meta*-isomer is slightly more stable than the *para*-isomer. Notwithstanding subtle variations in the C—H···O and C—H···π hydrogen bonding patterns, thermal motion analysis and molecular dynamics studies on periodic minicrystals of the two isomers suggest that preferred librational or conformational changes in the *meta*-isomer with respect to the *para*-isomer lead to its higher melting-point.

In conclusion, is it fair to invoke the *meta–para* melting-point rule for the anisylpinacolones? Most of the sets of compounds where this rule 'works' have simpler and smaller substituents than those present in the title compounds, whose molecular symmetry is the same, namely C_1. The phenyl group does not constitute a dominating portion of molecules **1** and **2** and, in this sense, qualitative arguments to the effect that a *para*-isomer packs more efficiently than its *meta* counterpart may be somewhat simplistic. The present study confirms that melting is a complex event and that careful analysis of the various enthalpic and entropic effects that take place just before and at the melting-point need to be dissected out carefully to obtain a clearer understanding of this important phenomenon.

Acknowledgements

Thanks are due to the UGC for fellowship support (S.S.K.), to Dr K. V. Raghavan and Dr J. S. Yadav for encouragement (J.A.R.P.S.), to Dr A. Nangia for the synthesis of the compounds studied, to Molecular Simulations for their cooperation (G.R.D.) and to the NIH for grant CA10925 (A.K.K., H.C.C.).

The CCDC CIF submission reference numbers are CCDC 146709 (*meta* isomer) and CCDC 146710 (*para* isomer).

REFERENCES

1. Ubbelohde R. *The Molten State of Matter*. Wiley: Chichester, 1978.
2. Gavezzotti A. *J. Chem. Soc., Perkin Trans. 2* 1995; 1399–1404.
3. Bondi A. *Physical Properties of Molecular Crystals, Liquids and Glasses*. Wiley: New York, 1968.
4. Scamehorn R, Bunnett J. *J. Org. Chem.* 1979; **44**: 2604–2608.

5. Sheldrick GM. SHELX97, Program for Crystal Structure Solution and Refinement. University of Göttingen: Göttingen, 1997.
6. Spek AL. PLATON, Program for Display and Analysis of Crystal and Molecular Structures. University of Utrecht: Utrecht, 1980–99.
7. Dunitz JD, Schomaker V, Trueblood KN. *J. Phys. Chem.* 1988; **92**: 856–867.
8. Mayo SL, Olafson BD, Goddard WA III. *J. Phys. Chem.* 1990; **94**: 8897–8909.
9. Desiraju GR, Steiner T. *The Weak Hydrogen Bond In Structural Chemistry and Biology*. Oxford University Press: Oxford, 1999.
10. Stewart JJP. MOPAC (Version 6.0). A General Molecular Orbital Package. Quantum Chemistry Program Exchange (QCPE 455), Department of Chemistry, Indiana University: Bloomington, IN.
11. Sarma JARP, Chaudhuri B, Desiraju GR. *Indian J. Chem., Sect. A* 2000; **39**: 253–261.
12. Gavezzotti A (ed). *Theoretical Aspects and Computer Modeling of the Molecular Solid State*. Wiley: Chichester. 1997.
13. Harder S. *Chem. Eur. J.* 1999; **5**: 1852–1861.
14. Desiraju GR. *Acc. Chem. Res.* 1996; **29**: 441–449.

